

1 Nitrogen Fixation in Arctic Coastal Waters (Qeqertarsuaq, West 2 Greenland): Influence of Glacial Melt on Diazotrophs, Nutrient 3 Availability, and Seasonal Blooms

4 Schlangen Isabell¹, Leon-Palmero Elizabeth^{1,2}, Moser Annabell¹, Xu Peihang¹, Laursen Erik¹, and
5 Löscher Carolin R.^{1,3}

6 ¹Nordceee, Department of Biology, University of Southern Denmark, Campusvej 55, 5230 Odense M, Denmark

7 ²Department of Geosciences, Princeton University, Princeton, New Jersey

8 ³DIAS, University of Southern Denmark, Odense, Denmark

9 **Correspondence:** Carolin R. Löscher (cloescher@biology.sdu.dk)

10
11 **Abstract.** The Arctic Ocean is undergoing rapid transformation due to climate change, with decreasing sea ice contributing to
12 a predicted increase in primary productivity. A critical factor determining future productivity in this region is the availability
13 of nitrogen, a key nutrient that often limits biological growth in Arctic waters. The fixation of dinitrogen (N₂) gas, a biological
14 process mediated by diazotrophs, provides a source of new nitrogen to marine ecosystems and has been increasingly recognized
15 as a potential contributor to nitrogen supply in the Arctic Ocean. Historically it was believed to be limited to oligotrophic
16 tropical and subtropical oceans, Arctic N₂ fixation has only garnered significant attention over the past decade, leaving a
17 gap in our understanding of its magnitude, the diazotrophic community, and potential environmental drivers. In this study, we
18 investigated N₂ fixation rates and the diazotrophic community in Arctic coastal waters, using a combination of isotope labeling,
19 genetic analyses and biogeochemical profiling, in order to explore its response to glacial meltwater, nutrient availability and
20 its impact on primary productivity. We observed N₂ fixation rates ranging from 0.16 to 2.71 nmol N L⁻¹ d⁻¹, notably higher than
21 many previously reported rates for Arctic waters. The diazotrophic community was predominantly composed of UCYN-A. The
22 highest N₂ fixation rates co-occurred with peaks in chlorophyll *a* and primary production at a station in the Vaigat Strait, likely
23 influenced by glacial meltwater input. On average, N₂ fixation contributed 1.6% of the estimated nitrogen requirement of primary
24 production, indicating that while its role is modest, it may still represent a nitrogen source in certain conditions. These findings
25 illustrate the potential importance of N₂ fixation in an environment previously not considered important for this process and
26 provide insights into its response to the projected melting of the polar ice cover.

27 28 1 Introduction

29
30 Nitrogen is a key element for life and often acts as a growth-limiting factor for primary productivity (Gruber and Sarmiento,
31 1997; Gruber, 2004; Gruber and Galloway, 2008). Despite nitrogen gas (N₂) making up approximately 78% of the atmosphere,
32 it remains inaccessible to most marine life forms. Diazotrophs, which are specialized bacteria and archaea, have the ability to
33 convert N₂ into biologically available nitrogen, facilitated by the nitrogenase enzyme complex carrying out the process of
34 biological nitrogen fixation (N₂ fixation) (Capone and Carpenter (1982)). Despite the fact that these organisms are highly spe-

35 cialized and N₂ fixation is energetically demanding, the ability to carry out this process is widespread amongst prokaryotes.
36 However, it is controlled by several factors such as temperature, light, nutrients and trace metals such as iron and molybdenum
37 (Sohm et al., 2011; Tang et al., 2019). Oceanic N₂ fixation is the major source of nitrogen to the marine system (Karl et al.,
38 2002; Gruber and Sarmiento, 1997), thus, diazotrophs determine the biological productivity of our planet (Falkowski et al.
39 (2008), impact the global carbon cycle and the formation of organic matter (Galloway et al., 2004; Zehr and Capone, 2020).
40 Traditionally it has been believed that the distribution of diazotrophs was limited to warm and oligotrophic waters (Buchanan
41 et al., 2019; Sohm et al., 2011; Luo et al., 2012) until putative diazotrophs were identified in the central Arctic Ocean and
42 Baffin Bay (Farnelid et al., 2011; Damm et al., 2010). First rate measurements have been reported for the Canadian Arctic by
43 Blais et al. (2012) and recent studies have reported rate measurements in adjacent seas (Harding et al., 2018; Sipler et al., 2017;
44 Shiozaki et al., 2017, 2018), drawing attention to cold and temperate waters as significant contributors to the global nitrogen
45 budget through diverse organisms.

46 UCYN-A has been described as the dominant active N₂ fixing cyanobacterial diazotroph in arctic waters (Harding et al.
47 (2018)), while other cyanobacteria have only occasionally been reported (Díez et al., 2012; Fernández-Méndez et al., 2016; Blais
48 et al.,) However, other recent studies suggest, that the majority of the arctic marine diazotrophs are NCDs (non-cyanobacterial
49 diazotroph) and those may contribute significantly to N₂ fixation in the Arctic Ocean (Shiozaki et al., 2018; Fernández-Méndez
50 et al., 2016; Harding et al., 2018; Von Friesen and Rie- mann, 2020). Recent work by Robicheau et al. (2023) nearby Baffin Bay,
51 geographically close to the sampling area, document low *nifH* gene abundance while still detecting diazotrophs in Arctic surface waters,
52 highlighting the patchy distribution of diazotrophs across Arctic coastal environments. Studies on the Arctic diazotroph community
53 remain scarce, leaving Arctic environments poorly understood regarding N₂ fixation. Shao et al. (2023) note the impossibility
54 of estimating Arctic N₂ fixation rates due to the sparse spatial coverage, which currently represents only approximately 1 % of
55 the Arctic Ocean. Increasing data coverage in future studies will aid in better constraining the contribution of N₂ fixation to
56 the global oceanic nitrogen budget (Tang et al. (2019)).

57 The Arctic ecosystem is undergoing significant changes driven by rising temperatures and the accelerated melting of sea ice, a
58 trend predicted to intensify in the future (Arrigo et al., 2008; Hanna et al., 2008; Haine et al., 2015). These climate-driven shifts
59 have stimulated primary productivity in the Arctic by 57 % from 1998 to 2018, elevating nutrient demands in the Arctic Ocean
60 (Ardyna and Arrigo, 2020; Arrigo and van Dijken, 2015; Lewis et al., 2020). This increase is attributed to prolonged
61 phytoplankton growing seasons and expanding ice-free areas suitable for phytoplankton growth (Arrigo et al. (2008)).
62 However, despite these dramatic changes, the role of N₂ fixation in sustaining Arctic primary production remains poorly
63 understood. While recent studies suggest that diazotrophic activity may contribute to nitrogen inputs in polar regions (Sipler
64 et al. (2017)), fundamental uncertainties remain regarding the extend, distribution and environmental drivers of N₂ Fixation in
65 the Arctic Ocean. Specifically, it is unclear whether increased glacial meltwater input enhances or inhibits N₂ Fixation through
66 changes in nutrient availability, stratification, and microbial community composition. Thus, the question of whether nitrogen
67 limitation will emerge as a key factor constraining Arctic primary production under future climate scenarios remains unresolved. In this
68 study, we investigate the diversity of diazotrophic communities alongside in situ N₂ fixation rate measurements in Disko Bay

(Qeqertarsuaq), a coastal Arctic system strongly influenced by glacial meltwater input. By linking environmental parameters to N₂ fixation dynamics, we aim to clarify the role of diazotrophs in Arctic nutrient cycling and assess their potential contribution to sustaining primary production in a changing Arctic. Understanding these processes is essential for refining biogeochemical models and predicting ecosystem responses to future climate change.

2 Material and methods

2.1 Seawater sampling

The research expedition was conducted from August 16 to 26 in 2022 aboard the Danish military vessel P540 within the waters of Qeqertarsuaq, located in the western region of Greenland (Kalaallit Nunaat). Discrete water samples were obtained using a 10 L Niskin bottle, manually lowered with a hand winch to five distinct depths (surface, 5, 25, 50, and 100 m). A comprehensive sampling strategy was employed at 10 stations (Fig. 1), covering the surface to a depth of 100 m. The sampled parameters included water characteristics, such as nutrient concentrations, chl *a*, particulate organic carbon (POC) and nitrogen (PON), molecular samples for nucleic acid extractions (DNA), dissolved inorganic carbon (DIC) as well as CTD sensor data. At three selected stations (3,7,10) N₂ fixation and primary production rates were quantified through concurrent incubation experiments. Samples for nutrient analysis, nitrate (NO₃⁻), nitrite (NO₂⁻) and phosphate (PO₄³⁻) were taken in triplicates, filtered through a 0.22 μ m syringe filter (Avantor VWR® Radnor, Pa, USA) and stored at -20 °C until further analysis. Concentrations were spectrophotometrically determined (Thermo Scientific, Genesys 1OS UV-VIS spectrophotometer) following the established protocols of Murphy and Riley (1962) for PO₄³⁻; García-Robledo et al. (2014) for NO₃⁻ & NO₂⁻ (detection limits: 0.01 μ mol L⁻¹ (NO₃⁻, NO₂⁻, and PO₄³⁻), 0.05 μ mol L⁻¹ (NH₄⁺)). Chl *a* samples were filtered onto 47 mm ø GF/F filters (GE Healthcare Life Sciences, Whatman, USA), placed into darkened 15 mL LightSafe centrifuge tubes (Merck, Rahway, NJ, USA) and were subsequently stored at -20 °C until further analysis. To determine the Chl *a* concentration, the samples were immersed in 8 mL of 90 % acetone overnight at 5 °C. Subsequently, 1 mL of the resulting solution was transferred to a 1.5 mL glass vial (Mikrolab Aarhus A/S, Aarhus, Denmark) the following day and subjected to analysis using the Trilogy® Fluorometer (Model #7200-00) equipped with a Chl *a* in vivo blue module (Model #7200-043, both Turner Designs, San Jose, CA, USA). Measurements of serial dilutions from a 4 mg L⁻¹ stock standard and 90 % acetone (serving as blank) were performed to calibrate the instrument. In addition, measurements of a solid-state secondary standard were performed every 10 samples. Water (1 L) water from each depth was filtered for the determination of POC and PON concentrations, as well as natural isotope abundance (δ ¹³C POC / δ ¹⁵N PON) using 47 mm ø, 0.7 μ m nominal pore size precombusted GF/F filter (GE Healthcare Life Sciences, Whatman, USA), which were subsequently stored at -20 °C until further analysis. Seawater samples for DNA were filtered through 47 mm ø, 0.22 μ m MCE membrane filter (Merck, Millipore Ltd., Ireland) for a maximum of 20 minutes, employing a gentle vacuum (200 mbar). The filtered volumes varied depending on the amount of material captured on the filter, ranging from 1.3 L to 2 L, with precise measurements recorded. The filters were promptly stored at -20 °C on the ship and moved to -80 °C upon arrival to the lab until further analysis.

104 To achieve detailed vertical profiles, a conductivity-temperature-depth-profiler (CTD, Seabird X) equipped with supplemen-
105 tary sensors for dissolved oxygen (DO), photosynthetic active radiation (PAR), and fluorescence (Fluorometer) was manually
106 deployed.

107 **2.2 Nitrogen fixation and primary production**

108 Water samples were collected at three distinct depths (0, 25 and 50 m) for the investigation of N₂ fixation rates and primary
109 production rates, encompassing the euphotic zone, chlorophyll maximum, and a light-absent zone. Three incubation stations
110 (Fig. 2: station 3, 7, 10) were chosen, in a way to cover the variability of the study area. This strategic sampling aimed to
111 capture a gradient of the water column with varying environmental conditions, relevant to the aim of the study. N₂ fixation
112 rates were assessed through triplicate incubations employing the modified ¹⁵N-N₂ dissolution technique after Großkopf et al.
113 (2012) and Mohr et al. (2010).

114 To ensure minimal contamination, 2.3 L glass bottles (Schott-Duran, Wertheim, Germany) underwent pre-cleaning and acid
115 washing before being filled with seawater samples. Oxygen contamination during sample collection was mitigated by gently
116 and bubble-free filling the bottles from the bottom, allowing the water to overflow. Each incubation bottle received a 100 mL
117 amendment of ¹⁵N-N₂ enriched seawater (98 %, Cambridge Isotope Laboratories, Inc., USA) achieving an average dissolved
118 N₂ isotope abundance (¹⁵N atom %) of 3.90 ± 0.02 atom % (mean \pm SD). Additionally, 1 mL of H¹³CO₃ (1 g/50 mL) (Sigma-
119 Aldrich, Saint Louis Missouri US) was added to each incubation bottle, roughly corresponding to 10 atom % enrichment and
120 thus measurements of primary production and N₂ fixation were conducted in the same bottle. Following the addition of both
121 isotopic components, the bottles were closed airtight with septa-fitted caps and incubated for 24 hours on-deck incubators with
122 a continuous surface seawater flow. These incubators, partially shaded (using daylight-filtering foil) to simulate in situ
123 photosynthetically active radiation (PAR) conditions, aimed to replicate environmental parameters experienced at the sampled
124 depths. Control incubations utilizing atmospheric air served as controls to monitor any natural changes in δ ¹⁵N not attributable
125 to ¹⁵N-N₂ addition. These control incubations were conducted using the dissolution method, like the ¹⁵N-N₂ enrichment
126 experiments, but with the substitution of atmospheric air instead of isotopic tracer.

127 After the incubation period, subsamples for nutrient analysis were taken from each incubation sample, and the remaining
128 content was subjected to the filtration process and were gently filtered (200 mbar) onto precombusted GF/F filters (Advantec,
129 47 mm ø, 0.7 μ m nominal pore size). This step ensured a comprehensive examination of both nutrient dynamics and the
130 isotopic composition of the particulate pool in the incubated samples. Samples were stored at -20 °C until further analysis.

131 Upon arrival in the lab, the filters were dried at 60 °C and to eliminate particulate inorganic carbon, subsequently subject to acid
132 fuming during which they were exposed to concentrated hydrochloric acid (HCL) vapors overnight in a desiccator. After
133 undergoing acid treatment, the filters were carefully dried, then placed into tin capsules and pelletized for subsequent analysis.
134 The determination of POC and PON, as well as isotopic composition (δ ¹³C POC / δ ¹⁵N PON), was carried out using an
135 elemental analyzer (Flash EA, ThermoFisher, USA) connected to a mass spectrometer (Delta V Advantage Isotope Ratio MS,
136 ThermoFisher, USA) with the ConFlo IV interface. This analytical setup was applied to all filters. These values, derived from
137

138 triplicate incubation measurements, exhibited no omission of data points or identification of outliers. Final rate calculations for N₂
139 fixation rates were performed after Mohr et al. (2010) and primary production rates after Slawyk et al. (1977). A detailed
140 sensitivity analysis for N₂ fixation rates and the contribution of each source of error of all parameters can be found as a
141 supplementary table.

142 **2.3 Molecular methods**

143
144 The filters were flash-frozen in liquid nitrogen, crushed and DNA was extracted using the Qiagen DNA/RNA AllPrep Kit (Qi-
145 agen, Hildesheim, DE), following the procedure outlined by the manufacturer. The concentration and quality of the extracted
146 DNA was assessed spectrophotometrically using a MySpec spectrofluorometer (VWR, Darmstadt, Germany). The prepara-
147 tion of the metagenome library and sequencing were performed by BGI (China). Sequencing libraries were generated using
148 MGIEasy Fast FS DNA Library Prep Set following the manufacturer's protocol. Sequencing was conducted with 2x150bp on
149 a DNBSEQ-G400 platform (MGI). SOAPnuke1.5.5 (Chen et al. (2018)) was used to filter and trim low quality reads and
150 adaptor contaminants from the raw sequence reads, as clean reads. In total, fifteen metagenomic datasets were produced with
151 an average of 9.6G bp per sample.

152 **2.3.1 Metagenomic De Novo assembly, gene prediction, and annotation**

153
154 Megahit v1.2.9 (Li et al. (2015)) was used to assemble clean reads for each dataset with its minimum contig length as 500.
155 Prodigal v2.6.3 (Hyatt et al. (2010)) with the setting of “-p meta” was then used to predict the open reading frames (ORFs) of
156 the assembled contigs. ORFs from all the available datasets were filtered (>100bp), dereplicated and merged into a catalog of
157 non-redundant genes using cd-hit-est (>95 % sequence identity) (Fu et al. (2012)). Salmon v1.10.0 (Patro et al. (2017)) with
158 the “– meta” option was employed to map clean reads of each dataset to the catalog of non-redundant genes and generate the
159 GPM (genes per million reads) abundance. EggNOG mapper v2.1.12 (Cantalapiedra et al. (2021)) was then performed to assign
160 KEGG Orthology (KO) and identify specific functional annotation for the catalog of non-redundant genes. The marker genes,
161 *nifDK* (K02586, K02591 nitrogenase molybdenum-iron protein alpha/beta chain) and *nifH* (K02588, nitrogenase iron protein),
162 were used for the evaluation of microbial potential of N₂ fixation. *RbcL* (K01601, ribulose-bisphosphate carboxylase large
163 chain) and *psbA* (K02703, photosystem II P680 reaction center D1 protein) were selected to evaluate the microbial potential
164 of carbon fixation and photosynthesis, respectively. The molecular datasets have been deposited with the accession number:
165 Bioproject PRJNA1133027.

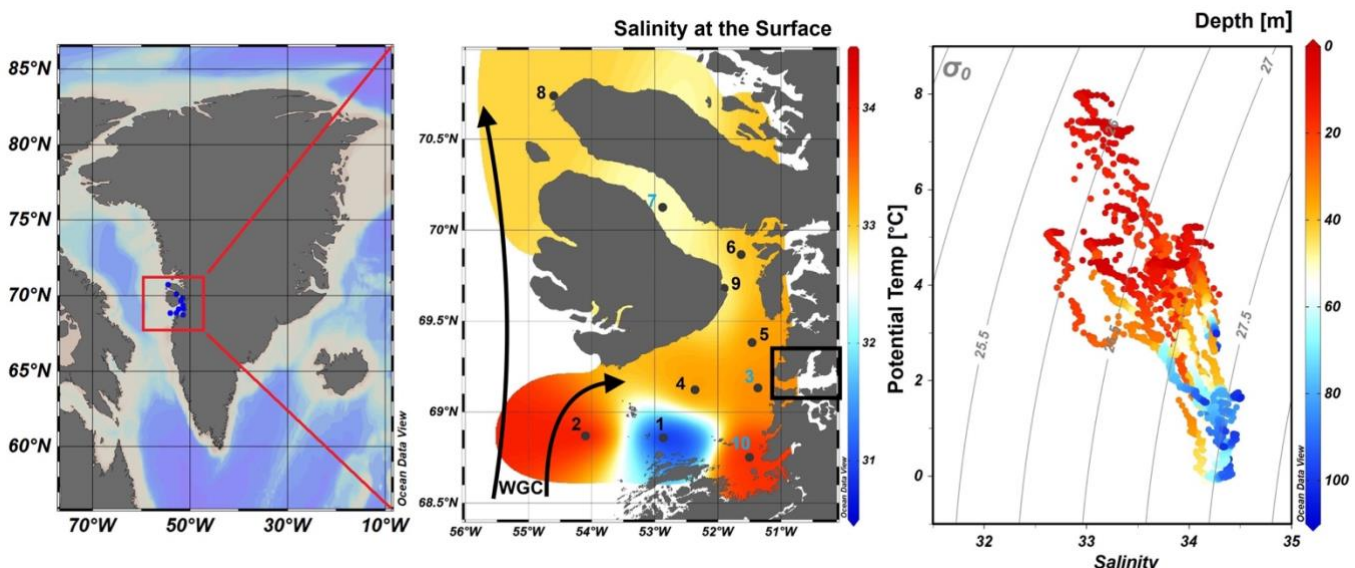
166 **3 Results and discussion**

167 **3.1 Hydrographic conditions in Qeqertarsuaq (Disco Bay) and Sullorsuaq (Vaigat) Strait**

168
169 Disko Bay (Qeqertarsuaq) is located along the west coast of Greenland (Kalaallit Nunaat) at approximately 69 °N (Figure 1),
170 and is strongly influenced by the West Greenland Current (WGC) which is associated with the broader Baffin Bay Polar Waters
171 (BBPW) (Mortensen et al., 2022; Hansen et al., 2012). The WGC does not only significantly shape the hydrographic conditions
172

173 within the bay but also plays an important role in the larger context of Greenland Ice Sheet melting (Mortensen et al. (2022)).
174 Central to the hydrographic system of the Qeqertarsuaq area is the Jakobshavn Isbræ, which is the most productive glacier in
175 the northern hemisphere and believed to drain about 7 % of the Greenland Ice Sheet and thus contributes substantially to the
176 water influx into the Qeqertarsuaq (Holland et al. (2008)). A predicted increased inflow of warm subsurface water, originating
177 from North Atlantic waters, has been suggested to further affect the melting of the Jakobshavn Isbræ and thus adds another
178 layer of complexity to this dynamic system (Holland et al., 2008; Hansen et al., 2012).

179 The hydrographic conditions in Qeqertarsuaq have a significant influence on biological processes, nutrient availability, and the

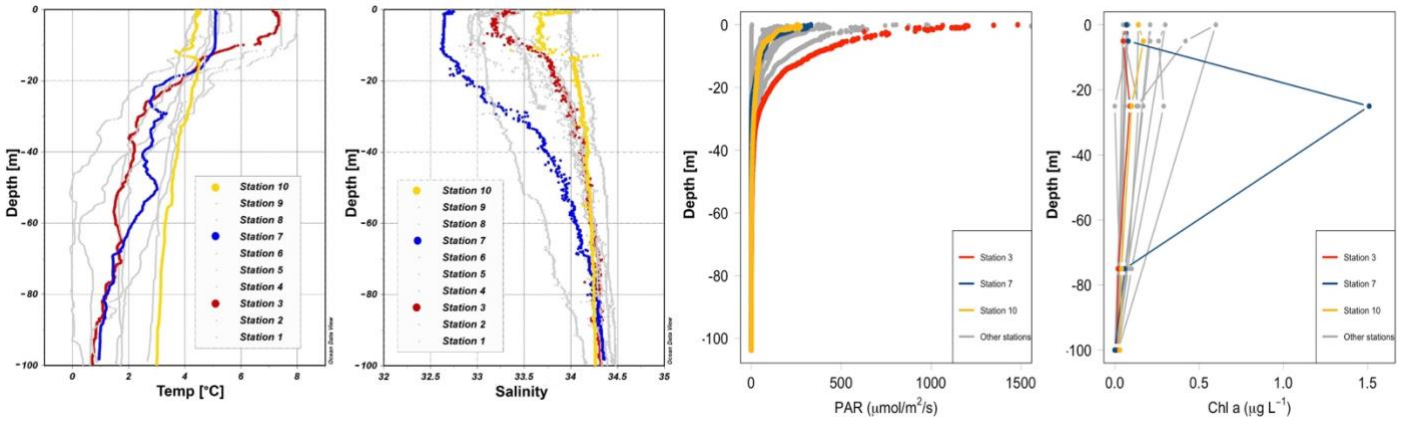


180
181 **Figure 1.** Map of Greenland (Kalaallit Nunaat) with indication of study area (red box), on the left. Interpolated distribution of Sea Surface
182 Salinity (SSS) values with corresponding isosurface lines and indication of 10 sampled stations (normal stations in black, incubation stations
183 in blue), black arrows indicate the West Greenland Current (WGC) and the black box indicate the location of the Jakobshavn Isbræ, in the
184 middle. Scatterplot of the potential temperature and salinity for all station data. The plot is used for the identification of the main water
185 masses within the study area. Isopycnals (kg m^{-3}) are depicted in grey lines, on the right. Figures were created in Ocean Data View (ODV)
186 (Schlitzer (2022)).

187 broader marine ecosystem (Munk et al., 2015; Hendry et al., 2019; Schiøtt, 2023).

188 During our survey, we found very heterogenous hydrographic conditions at the different stations across Qeqertarsuaq (Fig. 1 &
189 Fig. 2). The three selected stations for N_2 fixation analysis (stations 3, 7, and 10) were strategically chosen to capture the spatial
190 variability of the area. Surface salinity and temperature measurements at these stations indicate the influence of freshwater
191 input. The surface temperature exhibit a range of 4.5 to 8 °C, while surface salinity varies between 31 and 34, as illustrated in
192 Fig. 1. The profiles sampled during our survey extend to a maximum depth of 100 m. Comparison of temperature/salinity (T/S)
193 plots with recent studies suggests the presence of previously described water masses, including Warm Fjord Water (WFjW)
194

195 and Cold Fjord Water (CFjW) with an overlaying surface glacial meltwater runoff. Those water masses are defined with a
 196 density range of $27.20 \leq \sigma_0 \leq 27.31$ but different temperature profiles. Thus water masses can be differentiated by their
 197 temperature within the same density range (Gladish et al. (2015)). Other water masses like upper subpolar mode water
 198 (uSPMW), deep subpolar mode water (dSPMW) and Baffin Bay polar Water (BBPW) which has been identified in the Disko
 199 Bay (Qeqertarsuaq) before, cannot be identified from this data and may be present in deeper layers (Mortensen et al., 2022;
 200 Sherwood et al., 2021; Myers and Ribergaard, 2013; Rysgaard et al., 2020). The temperature and salinity profiles across the 10



201
 202
 203
Figure 2. Profiles of temperature (°C), salinity, photosynthetically active radiation (PAR) ($\mu\text{mol}/\text{m}^2/\text{s}$) and Chl *a* (mg m^{-3}) across stations 1 to
 204 10 with depth (m). Stations 3, 7, and 10 are highlighted in red, blue, and yellow, respectively, to emphasize incubation stations. Figures were
 205 created in Ocean Data View and R-Studio (Schlitzer (2022)).
 206

207 stations in the study area show distinct stratification and variability, which is represented through the three incubation stations
 208 (highlighted stations 3, 7, and 10 in Fig. 2). They display varying degrees of stratification and mixing, with notable differences
 209 in the salinity and temperature profiles. Station 3 and station 7 exhibit clear stratification in both temperature and salinity
 210 marked by the presence of thermoclines and haloclines. These features suggest significant freshwater input influenced by local
 211 weather conditions and climate dynamics, like surface heat absorption. In contrast, Station 10 exhibits a narrower range of
 212 temperature and salinity values throughout the water column compared to Stations 3 and 7, indicating more well-mixed
 213 conditions. This uniformity is likely influenced by the regional circulation pattern and partial upwelling (Hansen et al., 2012;
 214 Krawczyk et al., 2022). The distinct characteristics observed at station 10, as illustrated in the surface plot (Fig. 1), show an
 215 elevated salinity and colder temperatures compared

216 to the other stations. This feature suggests upwelling of deeper waters along the shallower shelf, likely facilitated by the local
 217 seafloor topography. Specifically, the seafloor shallowing off the coast of Station 10 may act as a barrier, disrupting typical
 218 circulation and forcing deeper, saltier, and colder waters to the surface. This pattern aligns with previous studies that describe
 219 similar mechanisms in the region (Krawczyk et al. (2022)). Their description of the bathymetry in Qeqertarsuaq, featuring
 220 depths ranging from ca. 50 to 900 m, suggests its impact on turbulent circulation patterns, leading to the mixing of different
 221

water masses. Evident variability in oceanographic conditions that can be observed throughout the study area occurs particularly along characteristic topographical features like steep slopes, canyons, and shallower areas. The summer melting of sea ice and glaciers introduces freshwater influxes that create distinct vertical and horizontal gradients in salinity and temperature in the Qeqertarsuaq area Hansen et al. (2012). Additionally, the accelerated melting of the Jakobshavn Isbraæ, influenced by the warmer inflow from the West Greenland Intermediate Current (WGIC), further alters the hydrographic conditions. Recent observations indicate significant warming and shoaling of the WGIC, potentially enabling it to overcome the sill separating the Ilulissat Fjord from the Qeqertarsuaq area (Hansen et al., 2012; Holland et al., 2008; Myers and Ribergaard, 2013). This shift intensifies glacier melting, driving substantial changes in the local ecological dynamics (Ardyna et al., 2014; Arrigo et al., 2008; Bhatia et al., 2013).

3.2 N₂ Fixation Rate Variability and Associated Environmental Conditions

We quantified N₂ fixation rates within the waters of Qeqertarsuaq, spanning from the surface to a depth of 50 m (Table 1). The rates ranged from 0.16 to 2.71 nmol N L⁻¹ d⁻¹ with all rates surpassing the minimum quantifiably rate (Appendix Table 1). Our findings represent rates at the upper range of those observed in the Arctic Ocean. Previous measurements in the region have been limited, with only one study in Baffin Bay by Blais et al. (2012), reporting rates of 0.02 nmol N L⁻¹ d⁻¹, which are 1-2 orders of magnitude lower than our observations. Moreover, Sipler et al. (2017), reported rates in the coastal Chukchi Sea, with average values of 7.7 nmol N L⁻¹ d⁻¹. These values currently represent some of the highest rates measured in Arctic shelf environments. Compared to these, our highest measured rate (2.71 nmol N L⁻¹ d⁻¹) is lower, but still important, particularly considering the more Atlantic-influenced location of our study site. Sipler et al. (2017) also noted that a significant fraction of diazotrophs were <3 µm in size, suggesting that small unicellular diazotrophs play a dominant role in Arctic nitrogen fixation. Altogether, our data contribute to the growing evidence that N₂ fixation is a widespread and potentially significant nitrogen source across various Arctic regions. Simultaneous primary production rate measurements ranged from 0.07 to 3.79 µmol N L⁻¹ d⁻¹, with the highest rates observed at station 7 and generally higher values in the surface layers. Employing Redfield stoichiometry, the measured N₂ fixation rates accounted for 0.47 to 2.6 % (averaging 1.57 %) of primary production at our stations. The modest contribution to primary production suggests that N₂ fixation does not exert a substantial influence on the productivity of these waters during the time of the sampling. Rather, our N₂ fixation rates suggest primary production to depend mostly on additional nitrogen sources including regenerated, meltwater or land based sources.

The N:P ratio, calculated as DIN to DIP, indicates a deficit in N for primary production based on Redfield stoichiometry (Fig. 3). This aligns with findings presented by Jensen et al. (1999) and Tremblay and Gagnon (2009), who observed a similar nitrogen limitation in this region. Such biogeochemical conditions would be expected to generate a niche for N₂ fixing organisms (Sohm et al. (2011)). While N₂ fixation did not chiefly sustain primary production during our sampling campaign, we hypothesize that N₂ fixation has the potential to play a role in bloom dynamics under certain conditions. As nitrogen availability decreases

during a bloom, it may provide a niche for N₂ fixation, potentially helping to extend the productive period of the bloom period

(Reeder et al. (2021)). Satellite data indicates that a fall bloom began in early August, following the annual spring bloom, as described by Ardyna et al. (2014). This double bloom situation may be driven by increased melting and the subsequent input of bioavailable nutrients and iron (Fe) from meltwater runoff (Arrigo et al., 2017; Hopwood et al., 2016; Bhatia et al., 2013). The meltwater from the Greenland Ice Sheet is a significant source of Fe (Bhatia et al., 2013; Hawkings et al., 2015, 2014), which is a limiting factor especially for diazotrophs (Sohm et al. (2011)). Consequently, it is plausible that Fe and nutrients from the Isbræ glacier create favorable conditions for both bloom development and diazotroph activity in Qeqertarsuaq. However, we emphasize that confirming a causal link between N_2 fixation and secondary bloom development requires further evidence, such as time-series data on nutrient concentrations, diazotroph abundance, and bloom dynamics.

Table 1. N_2 fixation ($\text{nmol N L}^{-1} \text{ d}^{-1}$), standard deviation (SD), primary productivity (PP; $\mu\text{mol C L}^{-1} \text{ d}^{-1}$), SD, percentage of estimated new primary productivity (% New PP) sustained by N_2 fixation, dissolved inorganic nitrogen compounds (NO_x), phosphorus (PO_4), and the molar nitrogen-to-phosphorus ratio (N:P) at stations 3, 7, and 10.

Station (no.)	Depth (m)	N_2 fixation ($\text{nmol N L}^{-1} \text{ d}^{-1}$)	SD (\pm)	Primary Productivity ($\mu\text{mol C L}^{-1} \text{ d}^{-1}$)	SD (\pm)	% New PP (%)	NO_x ($\mu\text{mol L}^{-1} \text{ d}^{-1}$)	PO_4 ($\mu\text{mol L}^{-1} \text{ d}^{-1}$)
3	0	1.20	0.21	0.466	0.08	1.71	0	0
3	25	1.88	0.11	0.588	0.04	2.11	0	0.70
3	50	0.29	0.01	0.209	0.00	0.91	0.33	1.48
7	0	2.49	0.44	0.63	0.20	2.60	0	0
7	25	2.71	0.22	3.79	2.45	0.47	0	0.45
7	50	0.53	0.24	0.33	0.36	1.08	0	0.97
10	0	1.48	0.12	0.74	0.15	1.33	0	0
10	25	0.31	0.01	0.29	0.07	0.73	0	0
10	50	0.16	0	0.07	0.07	1.40	0	0

A near-Redfield stoichiometry in POC:PON indicates that the particulate organic matter (POM) is freshly derived from an ongoing phytoplankton bloom, as phytoplankton generally assimilate carbon and nitrogen in relatively consistent proportions during active growth. In contrast, deviations from the Redfield ratio (e.g., elevated C:N or C:P) typically indicate microbial degradation and preferential remineralization of nitrogen and phosphorus (Redfield 1934; Geider and La Roche 2002; Sterner and Elser 2017). The absence of NO_x and the observed low N:P ratios suggest that nitrogen from earlier bloom phases has been largely depleted, potentially creating a niche for N_2 fixation as a supplementary nitrogen source. The onset and development of the bloom would be expected to lead to high nitrogen demands and intense competition for nitrogen sources. Notably, despite the apparent balance in the POM pool, the N:P ratio indicates strong nitrogen depletion and nutrient exhaustion within the ecosystem. This deficiency can be partly alleviated by N_2 fixation, providing possibly increasing amounts of nitrogen

over the course of the bloom. Moreover, DIP is generally limited in the environment (Table 1); however, some organisms may still access it through luxury phosphorus uptake, storing excess phosphate when it is sporadically available. A recent study by Laso Perez et al. (2024) documented changes in microbial community composition during an Arctic bloom, focusing on nitrogen cycling. They observed a shift from chemolithotrophic to heterotrophic organisms throughout the summer bloom and noted increased activity to compete for various nitrogen sources. However, no *nifH* gene copies, indicative of nitrogen-fixing organisms, were found in their dataset based on metagenome-assembled genomes (MAGs). This is not unexpected due to the classically low abundance of diazotrophs in marine microbial communities which has often been described (Turk-Kubo et al., 2015; Farnelid et al., 2019). Given the high productivity and metabolic activity observed in Qeqertarsuaq during a similar bloom period, the detected diazotrophs (Section 3.3) may play a more significant role than previously thought. Across the 10 stations there is considerable variability in POC and PON concentrations (Fig. 3). PON concentrations range from 0.0 $\mu\text{mol N L}^{-1}$ to 3.48 $\mu\text{mol N L}^{-1}$ (n=124), while POC concentrations range from 2.7 $\mu\text{mol C L}^{-1}$ to 27.2 $\mu\text{mol C L}^{-1}$ (n=144). The highest concentrations for both PON and POC were observed at station 7 at a depth of 25 m and coincide with the highest reported N_2 fixation rate (Figure Appendix A2 & A3). Generally, POC and PON concentrations decrease with depth, peaking at the deep chl *a* maximum (DCM), identified between 15 to 30 m across all stations. The DCM was identified based on measured chl *a* concentrations and previous descriptions in the region (Fox and Walker, 2022; Jensen et al., 1999). The variability in chl *a* concentrations indicates differences in phytoplankton abundance among the stations, with concentrations ranging between 0 to 0.42 mg m^{-3} . Excluding station 7, which exhibited the highest chl *a* concentration at the DCM (1.51 mg m^{-3}). While Tang et al. (2019) found that N_2 fixation measurements strongly correlated to satellite estimates of chl *a* concentrations, our results did not show a statistically significant correlation between nitrogen fixation rates and chl *a* concentrations overall (Figures A2 & A3). However, as noted, Station 7 at 25 m represents a unique case. The elevated concentration of chl *a* at this station likely resulted from a local phytoplankton bloom induced by meltwater outflow from the Isbræ glacier and sea ice melting, which may help explain the observed nitrogen fixation rates (Arrigo et al., 2017; Wang et al., 2014). This study's findings are in agreement with prior reports of analogous blooms occurring in the region ([Fox and Walker, 2022](#); [Jensen et al., 1999](#)).

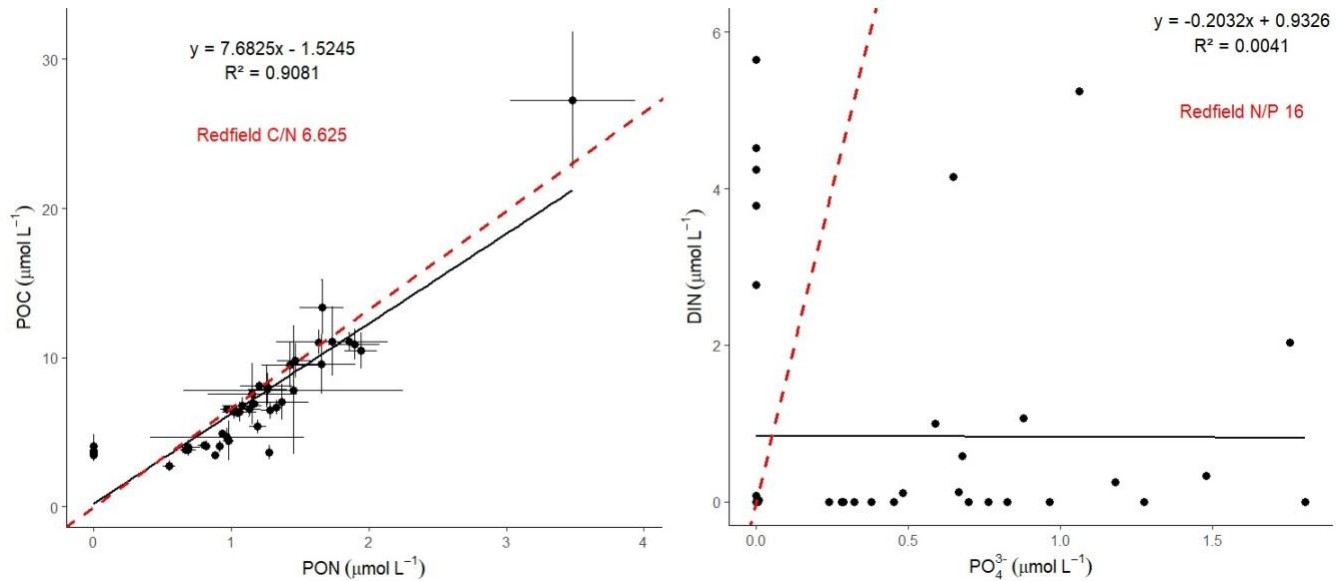


Figure 3. The POC/PON and DIN/DIP ratios at all 10 stations. The red line represents the Redfield ratios of POC/PON (106:16) and DIN/DIP (16:1).

3.3 Potential Contribution of UCYN-A to Nitrogen Fixation During a Diatom Bloom: Insights and Uncertainties

In our metagenomic analysis, we filtered the *nifH*, *nifD*, *nifK* genes, which code for the nitrogenase enzyme responsible for catalyzing N_2 fixation. We could identify sequences related to UCYN-A, which dominated the sequence pool of diazotrophs, particularly in the upper water masses (0 to 5 m) (Fig. 4). UCYN-A, a unicellular cyanobacterial symbiont, has a cosmopolitan distribution and is thought to substantially contribute to global N_2 fixation, as documented by (Martínez-Pérez et al., 2016; Tang et al., 2019). This conclusion is based on our metagenomic analysis, in which we set a sequence identity threshold of 95% for both *nif* and photosystem genes. Notably, we only recovered sequences related to UCYN-A within our *nif* sequence pool, suggesting its predominance among detected diazotrophs. However, metagenomic approaches may underestimate overall diazotroph diversity, and we cannot fully exclude the presence of other, less abundant diazotrophs that may have been missed using this method. While UCYN-A was primarily detected in surface waters, we also observed relatively high *nifK* values at S3_100m, an unusual finding given that UCYN-A is typically constrained to the euphotic zone. Previous studies have predominantly reported UCYN-A in surface waters; for instance Harding et al. (2018) and Shiozaki et al. (2017) detected UCYN-A exclusively in the upper layers of the Arctic Ocean. Additionally, Shiozaki et al. (2020) found UCYN-A2 at depths extending to the 0.1% light level but not below 66 m in the Chukchi Sea. The detection of UCYN-A at 100 m in our study suggests that alternative mechanisms, such as particle association, vertical transport, or local environmental conditions, may

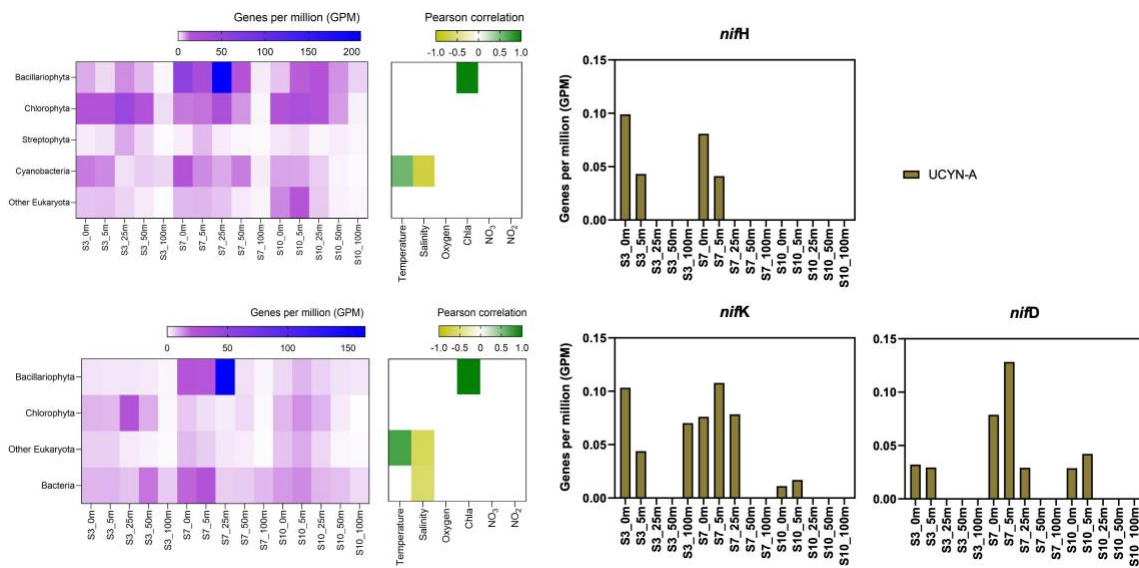
324 facilitate its presence at depth. Interestingly, despite very low *nifH* copy numbers being reported in nearby Baffin Bay by
325 Robicheau et al. (2023), UCYN-A dominated the metagenomic *nifH* community in our study, further underscoring this
326 organisms's presence in Arctic surface coastal areas under certain environmental conditions. This warrants further
327 investigation into the environmental drivers and potential processes enabling its occurrence in Arctic waters.

328 Due to the lack of genes such as those encoding Photosystem II and Rubisco, UCYN-A plays a significant role within the host
329 cell and participates in fundamental cellular processes. Consequently it has evolved to become a closely integrated component
330 of the host cell. Very recent findings demonstrate that UCYN-A imports proteins encoded by the host genome and has been
331 described as an early form of N₂ fixing organelle termed a "Nitroplast" (Coale et al. (2024)).

332 Previous investigations document that they are critical for primary production, supplying up to 85% of the fixed nitrogen to their
333 haptophyte host (Martínez-Pérez et al. (2016)). In addition to its high contribution to primary production, studies have shown
334 that UCYN-A in high latitude waters fix similar amounts of N₂ per cell as in the tropical Atlantic Ocean, even in nitrogen-
335 replete waters (Harding et al., 2018; Shiozaki et al., 2020; Martínez-Pérez et al., 2016; Krupke et al., 2015; Mills et al., 2020).
336 However, estimating their contribution to N₂ fixation in our study is challenging, particularly since we detected cyanobacteria
337 only at the surface but observe significant N₂ fixation rates below 5 m. The diazotrophic community is often underrepresented
338 in metagenomic datasets due to the low abundance of nitrogenase gene copies, implying our data does not present a complete
339 picture. We suspect a more diverse diazotrophic community exists, with UCYN-A being a significant contributor to N₂ fixation
340 in Arctic waters. However, the exact proportion of its contribution requires further investigation.

341 The contribution of N₂ fixation to carbon fixation (as percent of PP) is relatively low, at the time of our study. We identified
342 genes such as *rbcL*, which encodes Rubisco, a key enzyme in the carbon fixation pathway and *psbA*, a gene encoding
343 Photosystem II, involved in light-driven electron transfer in photosynthesis, in our metagenomic dataset. The gene *rbcL* (for the
344 carbon fixation pathway) and the gene *psbA* (for primary producers) were used to track the community of photosynthetic primary
345 producers in our metagenomic dataset. At station 7, elevated carbon fixation rates are correlated with high diatom
346 (*Bacillariophyta*) abundance and increased chl *a* concentration (Fig. 4), suggesting the onset of a bloom, which is also
347 observable via satellite images (Appendix A1). We hypothesize that meltwater, carrying elevated nutrient and trace metal
348 concentrations, was rapidly transported away from the glacier through the Vaigat Strait by strong winds, leading to increased
349 productivity, as previously described by Fox and Walker (2022) & Jensen et al. (1999). The elevated diatom abundance and
350 primary production rates at station 7 coincide with the highest N₂ fixation rates, which could possibly point toward a possible
351 diatom-diazotroph symbiosis (Foster et al., 2022, 2011; Schvarcz et al., 2022). However, we did not detect a clear diazotrophic
352 signal directly associated with the diatoms in our metagenomic dataset, which might be due to generally underrepresentation of
353 diazotrophs in metagenomes due to low abundance or low sequencing coverage. To investigate this further, we examined
354 the taxonomic composition of *Bacillariophyta* at higher resolution. Among the various abundant diatom genera,
355 *Rhizosolenia* and *Chaetoceros* have been identified as symbiosis with diazotrophs (Grosse, et al., 2010; Foster, et al.,
356 2010), representing less than 6% or 15% of *Bacillariophyta*, based on *rbcL* or *psbA*, respectively (Figure Appendix A4).
357 Although we underestimate diazotrophs to an extent, the presence of certain diatom-diazotroph symbiosis could help

358 explain the high nitrogen fixation rates in the diatom bloom to a certain degree. Compilation of *nif* sequences identified
 359 from this study as well as homologous from their NCBI top hit were added in Table S1. However, we cannot tell if the
 360 diazotrophs belong to UCYN-A1 or UCYN-A2, or UCYN-A3. Based on the Pierella Karlusich et al. (2021), they
 361 generated clonal *nifH* sequences from Tara Oceans, which the length of *nifH* sequences is much shorter than the two
 362 *nifH* sequences we generated in our study. Also, the available UCYN-A2 or UCYN-A3 *nifH* sequences from NCBI were
 363 shorter than the two *nifH* sequences we generated. Therefore, it would be not accurate to assign the *nifH* sequences to
 364 either group under UCYN-A. Furthermore, not much information is available regarding the different groups of UCYN-
 365 A using marker genes of *nifD* and *nifK*.
 366



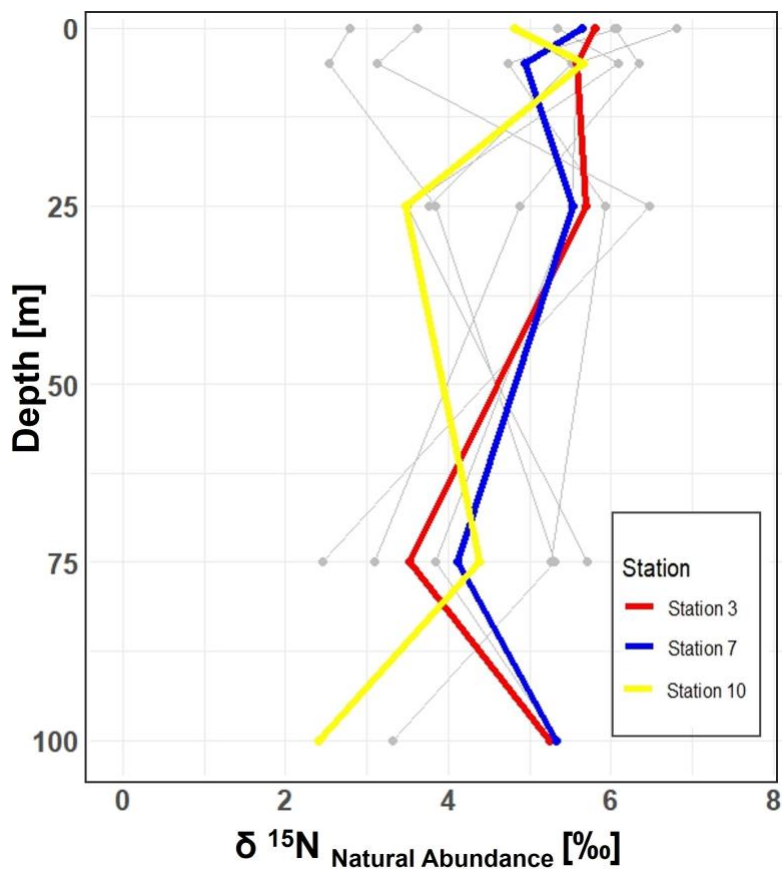
367
 368 **Figure 4.** Upper left image: *psbA* with correlation plot. Lower left image: *rbcL* with correlation plot. Right image: *nifH*, *nifD*, *nifK* genes
 369 per million reads in the metagenomic datasets. All figures display molecular data from metagenomic dataset for all sampled depth of station
 370 3,7,10

373 There is evidence that UCYN-A have a higher Fe demand, with input through meltwater or river runoff potentially being
 374 advantageous to those organisms (Shiozaki et al., 2017, 2018; Cheung et al., 2022). Consequently, UCYN-A might play a
 375 more critical role in the future with increased Fe-rich meltwater runoff. UCYN-A can potentially fuel primary productivity by
 376 supplying nitrogen, especially with increased melting, nutrient inputs, and more light availability due to rising temperatures as-
 377 sociated with climate change. This predicted enhancement of primary productivity may contribute to the biological drawdown
 378 of CO₂, acting as a negative feedback mechanism. These projections are based on studies forecasting increased temperatures,
 379 melting, and resulting biogeochemical changes leading to higher primary productivity. However large uncertainties make pre-
 380 dictions very difficult and should be handled with care. Thus we can only hypothesize that UCYN-A might be coupled to these
 381

382 dynamics by providing essential nitrogen.

383 3.4 $\delta^{15}\text{N}$ Signatures in particulate organic nitrogen show no clear evidence of nitrogen fixation

384
385 Stable isotopic composition, expressed using the $\delta^{15}\text{N}$ notation, serve as indicators for understanding nitrogen dynamics
386 because different biogeochemical processes fractionate nitrogen isotopes in distinct ways (Montoya (2008)). However, it is
387 important to keep in mind that the final isotopic signal is a combination of all processes and an accurate distinction between
388 processes cannot be made. N_2 fixation tends to enrich nitrogenous compounds with lighter isotopes, producing OM with
389 isotopic values ranging approximately from -2 to +2 ‰ (Dähnke and Thamdrup (2013)). Upon complete remineralization and
390 oxidation, organic matter contributes to a reduction in the average δ -values in the open ocean (e.g. Montoya et al. (2002);
391 Emeis et al. (2010)). Whereas processes like denitrification and anammox preferentially remove lighter isotopes, leading to
392 enrichment in heavier isotopes and delta values up to -25 ‰.
393



394
395
396 **Figure 5.** Vertical profiles of $\delta^{15}\text{N}$ natural abundance signatures in PON across 10 stations in the study area. Incubation stations 3, 7, and 10
397 are highlighted in red, blue, and yellow, respectively. The figure shows variations in $\delta^{15}\text{N}$ signatures with depth at each station, providing

398 insight into nitrogen cycling in the study area.

399
400 Thus, $\delta^{15}\text{N}$ values help to identify different processes of the nitrogen cycle generally present in a system (Dähnke and Tham-
401 drup (2013)). In our study, the $\delta^{15}\text{N}$ values of PON from all 10 stations, range between 2.45 ‰ and 8.30 ‰ within the 0 to
402 100 m depth range, thus do not exhibit a clear signal indicative of N_2 fixation. This suggests that N_2 fixation may contributes
403 only a certain fraction to export production or that it might have begun to play a role in isotopic fractionation during later
404 stages of the bloom. However, due to the limited temporal resolution and lack of direct measurements of N sources over time,
405 we cannot confirm this dynamic. Additional data – including time-series isotopic profiles and turnover measurements of
406 subsurface nitrate and diazotroph activity – would be needed to establish a causal link between N_2 fixation and the observed
407 isotopic patterns in the bloom context. The composition of OM in the surface ocean is influenced by the nitrogen substrate and
408 the fractionation factor during photosynthesis. When nitrate is depleted in the surface ocean, the isotopic signature of OM
409 produced during photosynthesis will mirror that of the nitrogen substrate. This substrate can originate from either nitrate in the
410 subsurface or N_2 fixation. Notably, nitrate, the primary form of dissolved nitrogen in the open ocean, typically exhibits an
411 average stable isotope value of around

412 5 ‰. No fractionation occurs during photosynthesis because the nitrogen source is entirely taken up in the surface waters
413 (Sigman et al. (2009)). In Qeqertarsuaq, where similar conditions prevail, this suggests that factors other than N_2 fixation are
414 influencing the observed δ -values and POM is sustained by nitrogen sources from deeper subsurface waters, as observed in
415 earlier studies (Fox and Walker (2022)).

416 In the eastern Baffin Bay waters, Atlantic water masses serve as an important source of nitrate for sustaining primary produc-
417 tivity, which is also reflected in the nitrogen isotopic signature in this study (Sherwood et al. (2021)). The influx of Atlantic
418 waters, characterized by NO_3^- values of approximately 5 ‰, closely matches the $\delta^{15}\text{N}$ values of observed PON concentrations
419 in our study. This suggests that Atlantic-derived NO_3^- serves as a primary source of new nitrogen to the initial stages of bloom
420 development (Fox and Walker, 2022; Knies, 2022). The mechanisms through which subsurface nitrate reaches the euphotic
421 layer are not well understood. However, potential pathways include vertical migration of phytoplankton and physical mixing.
422 Subsequently, nitrogen undergoes rapid recycling and remineralization processes to meet the system's nitrogen demands
423 (Jensen et al. (1999)).

424
425 **4 Conclusion**

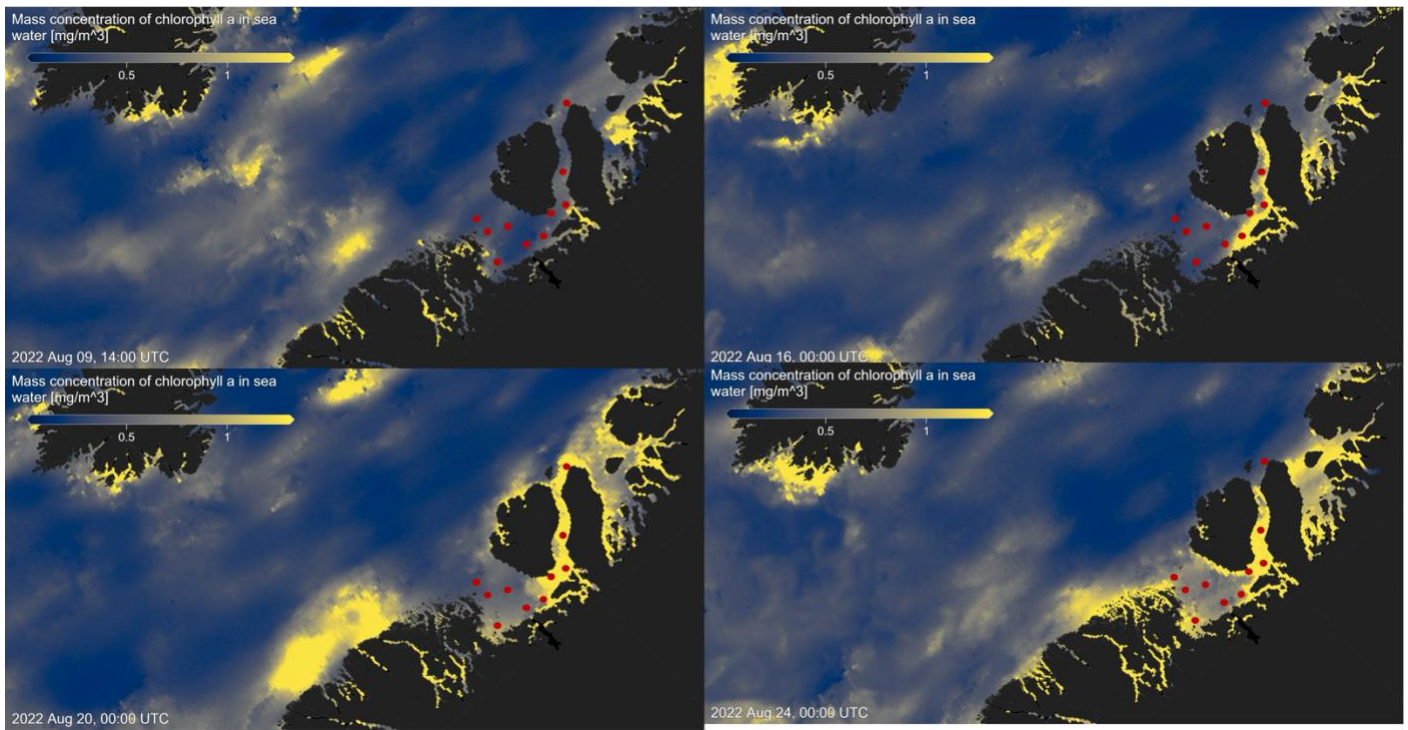
426
427 Our study highlights the occurrence of elevated rates of N_2 fixation in Arctic coastal waters, particularly prominent at station 7,
428 where they coincide with high chl a values, indicative of heightened productivity. Satellite observations tracing the origin of a
429 bloom near the Isbræ Glacier, subsequently moving through the Vaigat strait, suggest a recurring phenomenon likely triggered
430 by increased nutrient-rich meltwater originating from the glacier. This aligns with previous reports by Jensen et al. (1999) &
431 Fox and Walker (2022), underlining the significance of such events in driving primary productivity in the region. The contribu-
432 tion of N_2 fixation to primary production was low (average 1.57 %) across the stations. Since the demand was high relative to

433 the new nitrogen provided by N_2 fixation, the observed primary production must be sustained by the already present or adequate
434 amount of subsurface supply of NO_x nutrients in the seawater. This is also visible in the isotopic signature of the POM (Fox and
435 Walker, 2022; Sherwood et al., 2021). However, the detected N_2 fixation rates are likely linked to the development of the fresh
436 secondary summer bloom, which could be sustained by high nutrient and Fe availability from melting, potentially leading the
437 system into a nutrient-limited state. The ongoing high demand for nitrogen compounds may suggest an onset to further sustain
438 the bloom, but it remains speculative whether Fe availability definitively contributes to this process. The occurrence of such
439 double blooms has increased by 10 % in the Qeqertarsuaq and even 33 % in the Baffin Bay, with further projected increases
440 moving north from Greenland (Kalaallit Nunaat) waters (Ardyna et al. (2014)). Thus, nutrient demands are likely to increase,
441 and the role of N_2 fixation can become more significant. The diazotrophic community in this study is dominated by UCYN-A in
442 surface waters and may be linked to diatom abundance in deeper layers. This co-occurrence of diatoms and N_2 fixers in the
443 same location is probably due to the co-limitation of similar nutrients, rather than a symbiotic relationship. Thus, this highlights
444 the significant presence of diazotrophs despite their limited representation in datasets. It also highlights the potential for further
445 discoveries, as existing datasets likely underestimate the full extent of the diazotrophic community (Laso Perez et al., 2024;
446 Shao et al., 2023; Shiozaki et al., 2017, 2023). The reported N_2 fixation rates in the Vaigat strait within the Arctic Ocean are
447 notably higher than those observed in many other oceanic regions, emphasizing that N_2 fixation is an active and significant
448 process in these high-latitude waters. When compared to measured rates across various ocean systems using the ^{15}N approach,
449 the significance of these findings becomes clear. For instance, N_2 fixation rates are sometimes below the detection limit and
450 often relatively low ranging from 0.8 to 4.4 nmol N L⁻¹ d⁻¹ (Löscher et al., 2020, 2016; Turk et al., 2011). In contrast, higher
451 rates reach up to 20 nmol N L⁻¹ d⁻¹ (Rees et al. (2009)) and sometime exceptional high rates range from 38 to 610 nmol N L⁻¹
452 d⁻¹ (Bonnet et al. (2009)). The Arctic Ocean rates are thus significant in the global context, underscoring the region's role in
453 the global nitrogen cycle and the importance of N_2 fixation in supporting primary productivity in these waters.
454 These findings highlight the urgent need to understand the interplay between seasonal variations, sea-ice dynamics, and hydro-
455 graphic conditions in Qeqertarsuaq. As climate change accelerates the melting of the Greenland Ice Sheet at Jakobshavn Isbræ,
456 shifts in hydrodynamic patterns and hydrographic conditions in Qeqertarsuaq are anticipated. The resulting influx of warmer
457 waters could significantly reshape the bay's hydrography, making it crucial to comprehend the coupling of climate-driven
458 changes and oceanic processes in this vital Arctic region. Our study provides key insights into these dynamics and underscores
459 the importance of continued investigation to predict Qeqertarsuaq's future hydrographic state. By detailing the environmental
460 and hydrographic changes, we contribute valuable knowledge to the broader context of N_2 fixation in the Arctic Ocean. Given
461 nitrogen's pivotal role in Arctic ecosystem productivity, it is essential to explore diazotrophs, quantify N_2 fixation, and assess
462 their impact on ecosystem services as climate change progresses.

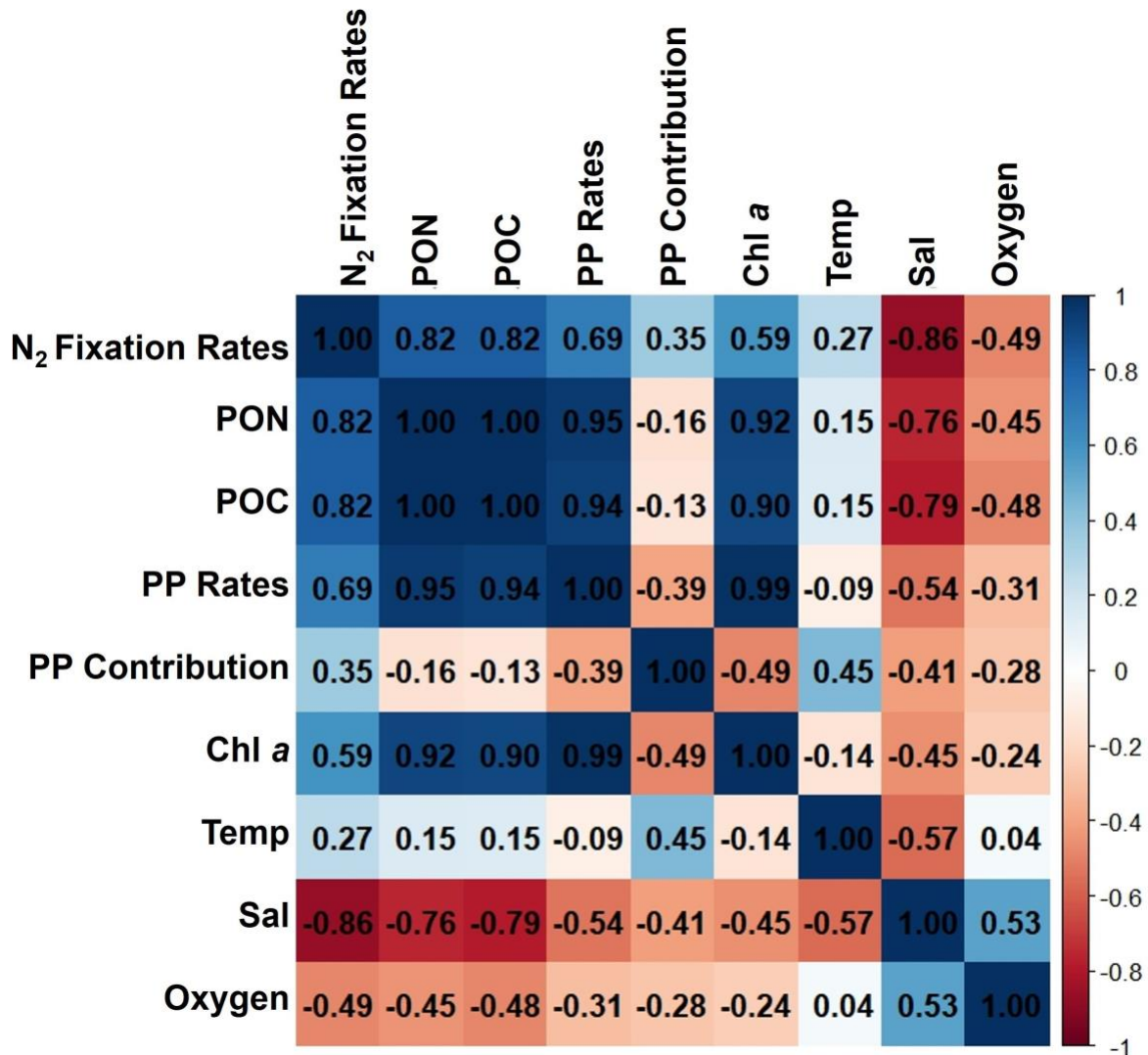
463 Appendix A

464

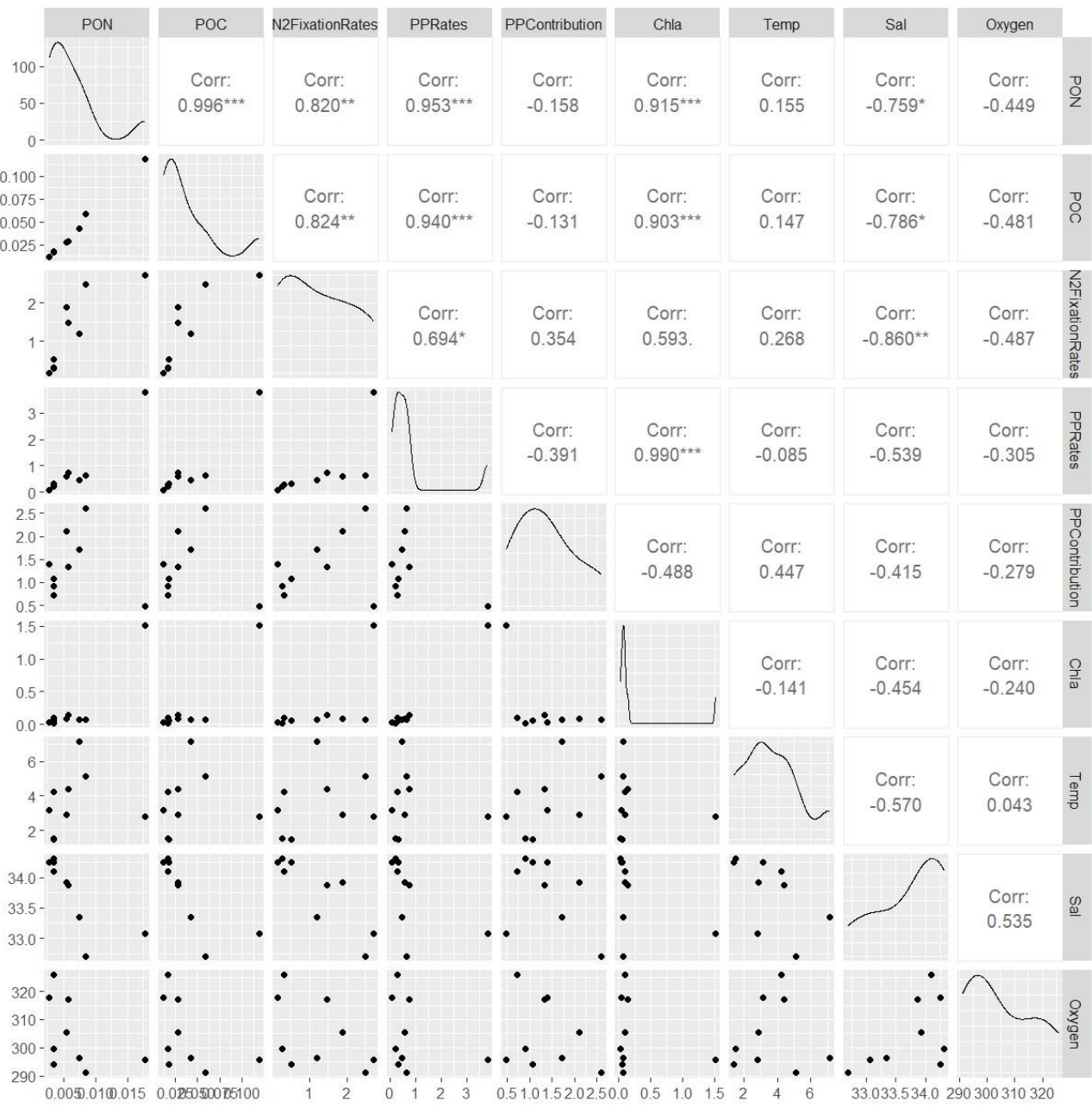
465



466
467 **Figure A1.** Chlorophyll a concentration mg m^{-3} at four time points before, during, and after sea water sampling in August 2022
468 (sampling stations indicated by red dots), obtained from MODIS-Aqua; <https://giovanni.gsfc.nasa.gov> (Aqua MODIS Global Mapped Chl a
469 Data, version R2022.0, DOI:10.5067/AQUA/MODIS/L3M/CHL/2022), 4 km resolution, last access 03 June 2024



470
471
472 **Figure A2.** Correlation matrix of environmental and biological variables. The plot shows the correlation coefficients between the following
473 parameters: N₂ fixation rates, PON, POC, PP rates, the contribution N₂ fixation to PP (PP contribution), Chl a, temperature (Temp), salinity
474 (Sal), and Oxygen. The scale ranges from -1 to 1, where values close to 1 or -1 indicate strong positive or negative correlations, respectively,
475 and values near 0 indicate weak or no correlation. The color intensity represents the strength and direction of the correlations, facilitating the
476 identification of relationships among the variables



477

478

479 **Figure A3.** This figure displays a ggpairs plot, showing pairwise relationships and correlations between biological and environmental variables. Pearson correlation coefficients displayed in the upper triangular panel, indicating the strength and significance of linear relationships. Statistical significance levels are indicated by stars (*), where * indicates $p < 0.05$, ** indicates $p < 0.01$ and *** indicates $p < 0.001$.

480

481

482

483

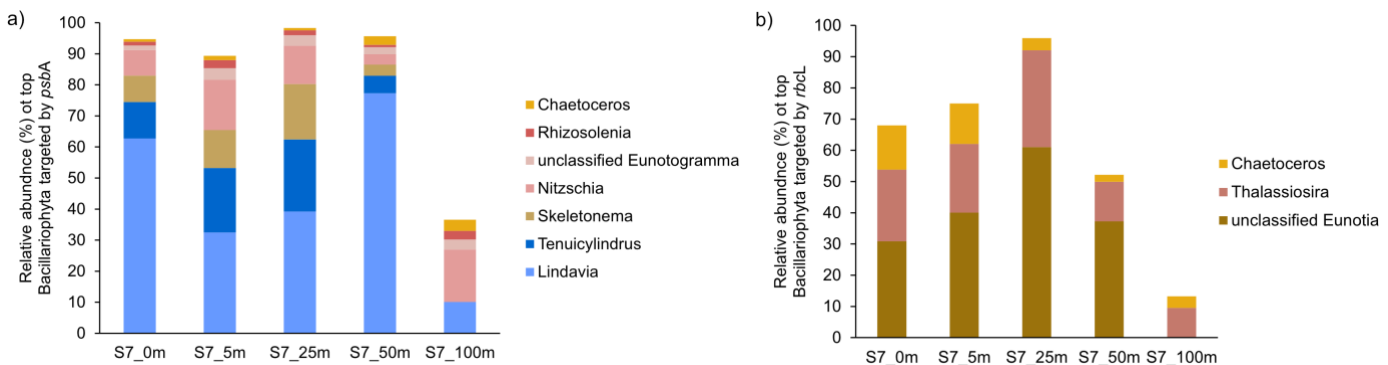


Figure A4 . Taxonomic composition of Bacillariophyta at Station 7 based on a) psbA and b) rbcL marker genes. The figure shows the relative abundance of Bacillariophyta genera detected in the metagenomic dataset, grouped by gene-specific classifications.

Station	Parameter (X)	Value	SD	$\delta\text{NFR}/\delta X$	Error contribution ($SD \times [\delta\text{NFR}/\delta X]^2$)	% Total error	Summary ($\text{nmol N L}^{-1} \text{d}^{-1}$)
3	Δt	1.00	0.00	0.00	0.00	0.00	Mean = 1.13 LOD = 0.73 MQR = 0.12
	A_{N2}	3.92%	0.00	0.00	0.00	0.00	
	A_{PNO}	0.370%	4.24×10^{-6}	2.63×10^6	2.46×10^2	29.49	
	A_{PNf}	0.420%	3.7×10^{-5}	2.36×10^5	3.03×10^2	35.54	
	$[PN]_f$	1.69×10^3	1.24×10^2	5.12×10^{-2}	3.21×10^2	34.97	
7	Δt	1.00	0.00	0.00	0.00	0.00	Mean = 1.92 LOD = 1.91 MQR = 0.47
	A_{N2}	3.92%	0.00	0.00	0.00	0.00	
	A_{PNO}	0.369%	4.0×10^{-6}	1.57×10^7	2.06×10^3	25.17	

	A_{PNf}	0.407%	5.47×10^{-5}	9.25×10^5	2.79×10^3	36.88	
	$[PN]_f$	4.62×10^3	8.2×10^2	6.77×10^{-2}	2.87×10^3	37.95	
10	Δt	1.00	0.00	0.00	0.00	0.00	Mean = 0.90 LOD = 0.96 MQR = 0.06
	A_{N2}	3.92%	0.00	0.00	0.00	0.00	
	A_{PNO}	0.371%	1.89×10^{-6}	-2.01×10^2	1.44×10^{-3}	31.24	
	A_{PNf}	0.371%	2.22×10^{-6}	2.01×10^2	2.05×10^{-3}	34.85	
	$[PN]_f$	5.91×10^2	1.89×10^2	-1.56×10^{-4}	3.69×10^{-3}	33.91	

490 *Appendix Table 1: Sensitivity analysis for N_2 fixation rates. The contribution of each source of error to the total uncertainty was determined and*
 491 *calculated after Montoya et al., (1996). Average values and standard deviations (SD) are provided for all parameters at each station. The partial*
 492 *derivative ($\delta NFR / \delta X$) of the N_2 fixation rate measurements is calculated for each parameter and evaluated using the provided average and*
 493 *standard deviation. The total and relative error are given for each parameter. Mean represents the average N_2 fixation rate measurement. MQR*
 494 *(minimal quantifiable rate) represents the total uncertainty linked to every measurement and is calculated using standard propagation of error.*
 495 *LOD (limit of detection) represents an alternative detection limit defined as $\Delta APN = 0.00146$.*

496
 497 *Data availability.* The presented data collected during the cruise will be made accessible on PANGEA. The molecular datasets have been
 498 deposited with the accession number: Bioproject PRJNA1133027

499
 500
 501
 502 *Author contributions.* IS carried out fieldwork and laboratory work at the University of Southern Denmark, and wrote the majority of the
 503 manuscript. ELP, AM, and EL conducted fieldwork and laboratory work at the University of Southern Denmark. PX performed metagenomic
 504 analysis and created the corresponding graphs. CRL designed the study, provided supervision and guidance throughout the project, and
 505 contributed to the writing and revision of the manuscript. All authors contributed to the conception of the study and participated in the writing
 506 and revision of the manuscript.

507
 508
 509
 510 *Competing interests.* The authors declare that they have no known competing financial interests or personal relationships that could have
 511 appeared to influence the work reported in this paper. One of the authors, CRL, serves as an Associate Editor for Biogeosciences.

512
 513
 514
 515 *Acknowledgements.* This work was supported by the Velux Foundation (grant no.29411 to Carolin R. Löscher) and through the DFF grant

516 from the the Independent Research Fund Denmark (grant no. 0217-00089B to Lasse Riemann, Carolin R. Löscher and Stig Markager). ELP
517 was supported by a postdoctoral contract from Danmarks Frie Forskningsfond (DFF, 1026-00428B) at SDU, and by a Marie Skłodowska-
518 Curie postdoctoral fellowship (HORIZON291 MSCA-2021-PF-01, project number: 101066750) by the European Commission at Princeton
519 University. We sincerely thank the captain and crew of the P540 during the cruise on the Danish military vessel for their invaluable support and
520 cooperation at sea. Our gratitude extends to Isaaffik Arctic Gateway for providing the infrastructure and opportunities that made this project
521 possible. We also acknowledge Zarah Kofoed for her technical support in the laboratory and thank all the Nordceee laboratory technicians for
522 their general assistance.

523 References

524

525 Ardyna, M. and Arrigo, K. R.: Phytoplankton dynamics in a changing Arctic Ocean, *Nature Climate Change*, 10, 892–903, 2020.

526 Ardyna, M., Babin, M., Gosselin, M., Devred, E., Rainville, L., and Tremblay, J.-É.: Recent Arctic Ocean sea ice loss triggers novel fall
527 phytoplankton blooms, *Geophysical Research Letters*, 41, 6207–6212, 2014.

528 Arrigo, K. R. and van Dijken, G. L.: Continued increases in Arctic Ocean primary production, *Progress in oceanography*, 136, 60–70, 2015.

529 Arrigo, K. R., van Dijken, G., and Pabi, S.: Impact of a shrinking Arctic ice cover on marine primary production, *Geophysical Research
530 Letters*, 35, 2008.

531 Arrigo, K. R., van Dijken, G. L., Castelao, R. M., Luo, H., Rennermalm, Å. K., Tedesco, M., Mote, T. L., Oliver, H., and Yager, P. L.:
532 Melting glaciers stimulate large summer phytoplankton blooms in southwest Greenland waters, *Geophysical Research Letters*, 44, 6278–
533 6285, 2017.

534 Bhatia, M. P., Kujawinski, E. B., Das, S. B., Breier, C. F., Henderson, P. B., and Charette, M. A.: Greenland meltwater as a significant and
535 potentially bioavailable source of iron to the ocean, *Nature Geoscience*, 6, 274–278, 2013.

536 Blais, M., Tremblay, J.-É., Jungblut, A. D., Gagnon, J., Martin, J., Thaler, M., and Lovejoy, C.: Nitrogen fixation and identification of
537 potential diazotrophs in the Canadian Arctic, *Global Biogeochemical Cycles*, 26, 2012.

538 Bonnet, S., Biegala, I. C., Dutrieux, P., Slemmons, L. O., and Capone, D. G.: Nitrogen fixation in the western equatorial Pacific: Rates,
539 diazotrophic cyanobacterial size class distribution, and biogeochemical significance, *Global Biogeochemical Cycles*, 23, 2009.

540 Buchanan, P. J., Chase, Z., Matear, R. J., Phipps, S. J., and Bindoff, N. L.: Marine nitrogen fixers mediate a low latitude pathway for
541 atmospheric CO₂ drawdown, *Nature Communications*, 10, 4611, 2019.

542 Cantalapiedra, C. P., Hernández-Plaza, A., Letunic, I., Bork, P., and Huerta-Cepas, J.: eggNOG-mapper v2: functional annotation, orthology
543 assignments, and domain prediction at the metagenomic scale, *Molecular biology and evolution*, 38, 5825–5829, 2021.

544 Capone, D. G. and Carpenter, E. J.: Nitrogen fixation in the marine environment, *Science*, 217, 1140–1142, 1982.

545 Chen, Y., Chen, Y., Shi, C., Huang, Z., Zhang, Y., Li, S., Li, Y., Ye, J., Yu, C., Li, Z., et al.: SOAPnuke: a MapReduce acceleration-supported
546 software for integrated quality control and preprocessing of high-throughput sequencing data, *Gigascience*, 7, gix120, 2018.

547 Cheung, S., Liu, K., Turk-Kubo, K. A., Nishioka, J., Suzuki, K., Landry, M. R., Zehr, J. P., Leung, S., Deng, L., and Liu, H.: High biomass
548 turnover rates of endosymbiotic nitrogen-fixing cyanobacteria in the western Bering Sea, *Limnology and Oceanography Letters*, 7, 501–
549 509, 2022.

550 Coale, T. H., Loconte, V., Turk-Kubo, K. A., Vanslembrouck, B., Mak, W. K. E., Cheung, S., Ekman, A., Chen, J.-H., Hagino, K., Takano,
551 Y., et al.: Nitrogen-fixing organelle in a marine alga, *Science*, 384, 217–222, 2024.

552 Dähnke, K. and Thamdrup, B.: Nitrogen isotope dynamics and fractionation during sedimentary denitrification in Boknis Eck, Baltic Sea,
553 *Biogeosciences*, 10, 3079–3088, 2013.

554 Damm, E., Helmke, E., Thoms, S., Schauer, U., Nöthig, E., Bakker, K., and Kiene, R.: Methane production in aerobic oligotrophic surface
555 water in the central Arctic Ocean, *Biogeosciences*, 7, 1099–1108, 2010.

556 Díez, B., Bergman, B., Pedrós-Alió, C., Antó, M., and Snoeijs, P.: High cyanobacterial *nifH* gene diversity in Arctic seawater and sea ice
557 brine, *Environmental microbiology reports*, 4, 360–366, 2012.

558 Emeis, K.-C., Mara, P., Schlarbaum, T., Möbius, J., Dähnke, K., Struck, U., Mihalopoulos, N., and Krom, M.: External N inputs and internal
559 N cycling traced by isotope ratios of nitrate, dissolved reduced nitrogen, and particulate nitrogen in the eastern Mediterranean Sea, *Journal*
560 *of Geophysical Research: Biogeosciences*, 115, 2010.

561 Falkowski, P. G., Fenchel, T., and Delong, E. F.: The microbial engines that drive Earth's biogeochemical cycles, *science*, 320, 1034–1039,
562 2008.

563 Farnelid, H., Andersson, A. F., Bertilsson, S., Al-Soud, W. A., Hansen, L. H., Sørensen, S., Steward, G. F., Hagström, Å., and Riemann, L.:
564 Nitrogenase gene amplicons from global marine surface waters are dominated by genes of non-cyanobacteria, *PloS one*, 6, e19 223, 2011.

565 Farnelid, H., Turk-Kubo, K., Ploug, H., Ossolinski, J. E., Collins, J. R., Van Mooy, B. A., and Zehr, J. P.: Diverse diazotrophs are present on
566 sinking particles in the North Pacific Subtropical Gyre, *The ISME journal*, 13, 170–182, 2019.

567 Fernández-Méndez, M., Turk-Kubo, K. A., Buttigieg, P. L., Rapp, J. Z., Krumpen, T., and Zehr, J. P.: Diazotroph diversity in the sea ice, melt
568 ponds, and surface waters of the Eurasian Basin of the Central Arctic Ocean, *Frontiers in microbiology*, 7, 217 140, 2016.

569 Foster, R. A., Goebel, N. L., & Zehr, J. P.: Isolation of *calothrix rhizosoleniae* (cyanobacteria) strain SC01 from *chaetoceros*
570 (bacillariophyta) spp. diatoms of the subtropical north pacific ocean 1. *Journal of Phycology*, 46(5), 1028-1037, 2010.

571 Foster, R. A., Kuypers, M. M., Vagner, T., Paerl, R. W., Musat, N., and Zehr, J. P.: Nitrogen fixation and transfer in open ocean diatom–
572 cyanobacterial symbioses, *The ISME journal*, 5, 1484–1493, 2011.

573 Foster, R. A., Tienken, D., Littmann, S., Whitehouse, M. J., Kuypers, M. M., and White, A. E.: The rate and fate of N₂ and C fixation by
574 marine diatom-diazotroph symbioses, *The ISME journal*, 16, 477–487, 2022.

575 Fox, A. and Walker, B. D.: Sources and Cycling of Particulate Organic Matter in Baffin Bay: A Multi-Isotope $\delta^{13}\text{C}$, $\delta^{15}\text{N}$, and $\Delta^{14}\text{C}$
576 Approach, *Frontiers in Marine Science*, 9, 846 025, 2022.

577 Fu, L., Niu, B., Zhu, Z., Wu, S., and Cd-hit, W. L.: Accelerated for clustering the next-generation sequencing data, *Bioinformatics*, 28,
578 3150–3152, 2012.

579 Galloway, J., Dentener, F., Capone, D., Boyer, E., Howarth, R., Seitzinger, S., Asner, G., Cleveland, C., Green, P., Holland, E., et al.: Nitrogen
580 cycles: past, present, and future. *Biogeochemistry* 70, 153e226, 2004.

581 García-Robledo, E., Corzo, A., and Papaspyrou, S.: A fast and direct spectrophotometric method for the sequential determination of nitrate
582 and nitrite at low concentrations in small volumes, *Marine Chemistry*, 162, 30–36, 2014.

583 Geider, R. J., & La Roche, J.: Redfield revisited: variability of C [ratio] N [ratio] P in marine microalgae and its biochemical
584 basis. *European Journal of Phycology*, 37(1), 1-17, 2002.

585 Gladish, C. V., Holland, D. M., and Lee, C. M.: Oceanic boundary conditions for Jakobshavn Glacier. Part II: Provenance and sources of
586 variability of Disko Bay and Ilulissat icefjord waters, 1990–2011, *Journal of Physical Oceanography*, 45, 33–63, 2015.

587 Grosse, J., Bombar, D., Doan, H. N., Nguyen, L. N., & Voss, M.: The Mekong River plume fuels nitrogen fixation and determines
588 phytoplankton species distribution in the South China Sea during low and high discharge season. *Limnology and Oceanography*, 55(4),
589 1668-1680, 2010.

590 Großkopf, T., Mohr, W., Baustian, T., Schunck, H., Gill, D., Kuypers, M. M., Lavik, G., Schmitz, R. A., Wallace, D. W., and LaRoche, J.:

591 Doubling of marine dinitrogen-fixation rates based on direct measurements, *Nature*, 488, 361–364, 2012.

592 Gruber, N.: The dynamics of the marine nitrogen cycle and its influence on atmospheric CO₂ variations, in: The ocean carbon cycle and
593 climate, pp. 97–148, Springer, 2004.

594 Gruber, N. and Galloway, J. N.: An Earth-system perspective of the global nitrogen cycle, *Nature*, 451, 293–296, 2008.

595 Gruber, N. and Sarmiento, J. L.: Global patterns of marine nitrogen fixation and denitrification, *Global biogeochemical cycles*, 11, 235–266,
596 1997.

597 Haine, T. W., Curry, B., Gerdes, R., Hansen, E., Karcher, M., Lee, C., Rudels, B., Spreen, G., de Steur, L., Stewart, K. D., et al.: Arctic
598 freshwater export: Status, mechanisms, and prospects, *Global and Planetary Change*, 125, 13–35, 2015.

599 Hanna, E., Huybrechts, P., Steffen, K., Cappelen, J., Huff, R., Shuman, C., Irvine-Fynn, T., Wise, S., and Griffiths, M.: Increased runoff from
600 melt from the Greenland Ice Sheet: a response to global warming, *Journal of Climate*, 21, 331–341, 2008.

601 Hansen, M. O., Nielsen, T. G., Stedmon, C. A., and Munk, P.: Oceanographic regime shift during 1997 in Disko Bay, western Greenland,
602 *Limnology and Oceanography*, 57, 634–644, 2012.

603 Harding, K., Turk-Kubo, K. A., Sipler, R. E., Mills, M. M., Bronk, D. A., and Zehr, J. P.: Symbiotic unicellular cyanobacteria fix nitrogen in
604 the Arctic Ocean, *Proceedings of the National Academy of Sciences*, 115, 13 371–13 375, 2018.

605 Hawkings, J., Wadham, J., Tranter, M., Lawson, E., Sole, A., Cowton, T., Tedstone, A., Bartholomew, I., Nienow, P., Chandler, D., et al.:
606 The effect of warming climate on nutrient and solute export from the Greenland Ice Sheet, *Geochemical Perspectives Letters*, pp. 94–104,
607 2015.

608 Hawkings, J. R., Wadham, J. L., Tranter, M., Raiswell, R., Benning, L. G., Statham, P. J., Tedstone, A., Nienow, P., Lee, K., and Telling, J.:
609 Ice sheets as a significant source of highly reactive nanoparticulate iron to the oceans, *Nature communications*, 5, 1–8, 2014.

610 Hendry, K. R., Huvenne, V. A., Robinson, L. F., Annett, A., Badger, M., Jacobel, A. W., Ng, H. C., Opher, J., Pickering, R. A., Taylor, M. L.,
611 et al.: The biogeochemical impact of glacial meltwater from Southwest Greenland, *Progress in Oceanography*, 176, 102 126, 2019.

612 Holland, D. M., Thomas, R. H., De Young, B., Ribergaard, M. H., and Lyberth, B.: Acceleration of Jakobshavn Isbræ triggered by warm
613 subsurface ocean waters, *Nature geoscience*, 1, 659–664, 2008.

614 Hopwood, M. J., Connolly, D. P., Arendt, K. E., Juul-Pedersen, T., Stinchcombe, M. C., Meire, L., Esposito, M., and Krishna, R.: Seasonal
615 changes in Fe along a glaciated Greenlandic fjord, *Frontiers in Earth Science*, 4, 15, 2016.

616 Hyatt, D., Chen, G.-L., LoCascio, P. F., Land, M. L., Larimer, F. W., and Hauser, L. J.: Prodigal: prokaryotic gene recognition and translation
617 initiation site identification, *BMC bioinformatics*, 11, 1–11, 2010.

618 Jensen, H. M., Pedersen, L., Burmeister, A., and Winding Hansen, B.: Pelagic primary production during summer along 65 to 72 N off West
619 Greenland, *Polar Biology*, 21, 269–278, 1999.

620 Karl, D., Michaels, A., Bergman, B., Capone, D., Carpenter, E., Letelier, R., Lipschultz, F., Paerl, H., Sigman, D., and Stal, L.: Dinitrogen
621 fixation in the world's oceans, *The nitrogen cycle at regional to global scales*, pp. 47–98, 2002.

622 Knies, J.: Nitrogen isotope evidence for changing Arctic Ocean ventilation regimes during the Cenozoic, *Geophysical Research Letters*, 49,
623 e2022GL099 512, 2022.

624 Krawczyk, D. W., Yesson, C., Knutz, P., Arboe, N. H., Blicher, M. E., Zinglersen, K. B., and Wagnholt, J. N.: Seafloor habitats across
625 geological boundaries in Disko Bay, central West Greenland, *Estuarine, Coastal and Shelf Science*, 278, 108 087, 2022.

626 Krupke, A., Mohr, W., LaRoche, J., Fuchs, B. M., Amann, R. I., and Kuypers, M. M.: The effect of nutrients on carbon and nitrogen fixation
627 by the UCYN-A–haptophyte symbiosis, *The ISME journal*, 9, 1635–1647, 2015.

628 Laso Perez, R., Rivas Santisteban, J., Fernandez-Gonzalez, N., Mundy, C. J., Tamames, J., and Pedros-Alio, C.: Nitrogen cycling during an
629 Arctic bloom: from chemolithotrophy to nitrogen assimilation, *bioRxiv*, pp. 2024–02, 2024.

630 Lewis, K., Van Dijken, G., and Arrigo, K. R.: Changes in phytoplankton concentration now drive increased Arctic Ocean primary production,
631 *Science*, 369, 198–202, 2020.

632 Li, D., Liu, C.-M., Luo, R., Sadakane, K., and Lam, T.-W.: MEGAHIT: an ultra-fast single-node solution for large and complex metagenomics
633 assembly via succinct de Bruijn graph, *Bioinformatics*, 31, 1674–1676, 2015.

634 Löscher, C. R., Bourbonnais, A., Dekaezemacker, J., Charoenpong, C. N., Altabet, M. A., Bange, H. W., Czeschel, R., Hoffmann, C., and
635 Schmitz, R.: N₂ fixation in eddies of the eastern tropical South Pacific Ocean, *Biogeosciences*, 13, 2889–2899, 2016.

636 Löscher, C. R., Mohr, W., Bange, H. W., and Canfield, D. E.: No nitrogen fixation in the Bay of Bengal?, *Biogeosciences*, 17, 851–864, 2020.

637 Luo, Y.-W., Doney, S., Anderson, L., Benavides, M., Berman-Frank, I., Bode, A., Bonnet, S., Boström, K. H., Böttjer, D., Capone, D., et al.:
638 Database of diazotrophs in global ocean: abundance, biomass and nitrogen fixation rates, *Earth System Science Data*, 4, 47–73, 2012.

639 Martínez-Pérez, C., Mohr, W., Löscher, C. R., Dekaezemacker, J., Littmann, S., Yilmaz, P., Lehnen, N., Fuchs, B. M., Lavik, G., Schmitz,
640 R. A., et al.: The small unicellular diazotrophic symbiont, UCYN-A, is a key player in the marine nitrogen cycle, *Nature Microbiology*, 1,
641 1–7, 2016.

642 Mills, M. M., Turk-Kubo, K. A., van Dijken, G. L., Henke, B. A., Harding, K., Wilson, S. T., Arrigo, K. R., and Zehr, J. P.: Unusual marine
643 cyanobacteria/haptophyte symbiosis relies on N₂ fixation even in N-rich environments, *The ISME Journal*, 14, 2395–2406, 2020.

644 Mohr, W., Grosskopf, T., Wallace, D. W., and LaRoche, J.: Methodological underestimation of oceanic nitrogen fixation rates, *PloS one*, 5,
645 e12 583, 2010.

646 Montoya, J. P.: Nitrogen stable isotopes in marine environments, *Nitrogen in the marine environment*, 2, 1277–1302, 2008.

647 Montoya, J. P., Carpenter, E. J., and Capone, D. G.: Nitrogen fixation and nitrogen isotope abundances in zooplankton of the oligotrophic
648 North Atlantic, *Limnology and Oceanography*, 47, 1617–1628, 2002.

649 Mortensen, J., Rysgaard, S., Winding, M., Juul-Pedersen, T., Arendt, K., Lund, H., Stuart-Lee, A., and Meire, L.: Multidecadal water mass
650 dynamics on the West Greenland Shelf, *Journal of Geophysical Research: Oceans*, 127, e2022JC018 724, 2022.

651 Munk, P., Nielsen, T. G., and Hansen, B. W.: Horizontal and vertical dynamics of zooplankton and larval fish communities during mid-
652 summer in Disko Bay, West Greenland, *Journal of Plankton Research*, 37, 554–570, 2015.

653 Murphy, J. and Riley, J. P.: A modified single solution method for the determination of phosphate in natural waters, *Analytica chimica acta*,
654 27, 31–36, 1962.

655 Myers, P. G. and Ribergaard, M. H.: Warming of the polar water layer in Disko Bay and potential impact on Jakobshavn Isbrae, *Journal of
656 Physical Oceanography*, 43, 2629–2640, 2013.

657 Patro, R., Duggal, G., Love, M. I., Irizarry, R. A., and Kingsford, C.: Salmon provides fast and bias-aware quantification of transcript
658 expression, *Nature methods*, 14, 417–419, 2017.

659 Redfield, A. C.: On the proportions of organic derivatives in sea water and their relation to the composition of plankton (Vol. 1). Liverpool:
660 university press of liverpool, 1934.

661 Reeder, C. F., Stoltenberg, I., Javidpour, J., and Löscher, C. R.: Salinity as a key control on the diazotrophic community composition in the
662 Baltic Sea, *Ocean Science Discussions*, 2021, 1–30, 2021.

663 Rees, A. P., Gilbert, J. A., and Kelly-Gerrey, B. A.: Nitrogen fixation in the western English Channel (NE Atlantic ocean), *Marine Ecology
664 Progress Series*, 374, 7–12, 2009.

665 Robicheau, B. M., Tolman, J., Rose, S., Desai, D., and LaRoche, J.: Marine nitrogen-fixers in the Canadian Arctic Gateway are dominated
666 by biogeographically distinct noncyanobacterial communities. *FEMS Microbiology Ecology*, 99(12), 122, 2023.

667 Rysgaard, S., Boone, W., Carlson, D., Sejr, M., Bendtsen, J., Juul-Pedersen, T., Lund, H., Meire, L., and Mortensen, J.: An updated view on
668 water masses on the pan-west Greenland continental shelf and their link to proglacial fjords, *Journal of Geophysical Research: Oceans*,
669 125, e2019JC015 564, 2020.

670 Schiøtt, S.: The Marine Ecosystem of Ilulissat Icefjord, Greenland, Ph.D. thesis, Department of Biology, Aarhus University, Denmark, 2023.

671 Schlitzer, R.: Ocean data view, 2022.

672 Schwarcz, C. R., Wilson, S. T., Caffin, M., Stancheva, R., Li, Q., Turk-Kubo, K. A., White, A. E., Karl, D. M., Zehr, J. P., and Steward, G. F.:
673 Overlooked and widespread pennate diatom-diazotroph symbioses in the sea, *Nature communications*, 13, 799, 2022.

674 Shao, Z., Xu, Y., Wang, H., Luo, W., Wang, L., Huang, Y., Agawin, N. S. R., Ahmed, A., Benavides, M., Bentzon-Tilia, M., et al.: Global
675 oceanic diazotroph database version 2 and elevated estimate of global N₂ fixation, *Earth System Science Data*, 15, 2023.

676 Sherwood, O. A., Davin, S. H., Lehmann, N., Buchwald, C., Edinger, E. N., Lehmann, M. F., and Kienast, M.: Stable isotope ratios in
677 seawater nitrate reflect the influence of Pacific water along the northwest Atlantic margin, *Biogeosciences*, 18, 4491–4510, 2021.

678 Shiozaki, T., Bombar, D., Riemann, L., Hashihama, F., Takeda, S., Yamaguchi, T., Ehama, M., Hamasaki, K., and Furuya, K.: Basin scale
679 variability of active diazotrophs and nitrogen fixation in the North Pacific, from the tropics to the subarctic Bering Sea, *Global Biogeochemical Cycles*, 31, 996–1009, 2017.

680 Shiozaki, T., Fujiwara, A., Ijichi, M., Harada, N., Nishino, S., Nishi, S., Nagata, T., and Hamasaki, K.: Diazotroph community structure and
681 the role of nitrogen fixation in the nitrogen cycle in the Chukchi Sea (western Arctic Ocean), *Limnology and Oceanography*, 63, 2191–
682 2205, 2018.

683 Shiozaki, T., Fujiwara, A., Inomura, K., Hirose, Y., Hashihama, F., and Harada, N.: Biological nitrogen fixation detected under Antarctic sea
684 ice, *Nature geoscience*, 13, 729–732, 2020.

685 Shiozaki, T., Nishimura, Y., Yoshizawa, S., Takami, H., Hamasaki, K., Fujiwara, A., Nishino, S., and Harada, N.: Distribution and survival
686 strategies of endemic and cosmopolitan diazotrophs in the Arctic Ocean, *The ISME journal*, 17, 1340–1350, 2023.

687 Sigman, D. M., DiFiore, P. J., Hain, M. P., Deutsch, C., Wang, Y., Karl, D. M., Knapp, A. N., Lehmann, M. F., and Pantoja, S.: The dual
688 isotopes of deep nitrate as a constraint on the cycle and budget of oceanic fixed nitrogen, *Deep Sea Research Part I: Oceanographic
689 Research Papers*, 56, 1419–1439, 2009.

690 Sipler, R. E., Gong, D., Baer, S. E., Sanderson, M. P., Roberts, Q. N., Mulholland, M. R., and Bronk, D. A.: Preliminary estimates of the
691 contribution of Arctic nitrogen fixation to the global nitrogen budget, *Limnology and Oceanography Letters*, 2, 159–166, 2017.

692 Slawyk, G., Collos, Y., and Auclair, J.-C.: The use of the ¹³C and ¹⁵N isotopes for the simultaneous measurement of carbon and nitrogen
693 turnover rates in marine phytoplankton 1, *Limnology and Oceanography*, 22, 925–932, 1977.

694 Sohm, J. A., Webb, E. A., and Capone, D. G.: Emerging patterns of marine nitrogen fixation, *Nature Reviews Microbiology*, 9, 499–508,
695 2011.

696 Sterner, R. W., & Elser, J. J. *Ecological stoichiometry: the biology of elements from molecules to the biosphere*. In *Ecological stoichiometry*.
697 Princeton university press, 2017.

698 Tang, W., Wang, S., Fonseca-Batista, D., Dehairs, F., Gifford, S., Gonzalez, A. G., Gallinari, M., Planquette, H., Sarthou, G., and Cassar, N.:
699 Revisiting the distribution of oceanic N₂ fixation and estimating diazotrophic contribution to marine production, *Nature communications*,
700 10, 831, 2019.

701

702 Tremblay, J.-É. and Gagnon, J.: The effects of irradiance and nutrient supply on the productivity of Arctic waters: a perspective on climate
703 change, in: *Influence of climate change on the changing arctic and sub-arctic conditions*, pp. 73–93, Springer, 2009.

704 Turk, K. A., Rees, A. P., Zehr, J. P., Pereira, N., Swift, P., Shelley, R., Lohan, M., Woodward, E. M. S., and Gilbert, J.: Nitrogen fixation and
705 nitrogenase (*nifH*) expression in tropical waters of the eastern North Atlantic, *The ISME journal*, 5, 1201–1212, 2011.

706 Turk-Kubo, K. A., Frank, I. E., Hogan, M. E., Desnues, A., Bonnet, S., and Zehr, J. P.: Diazotroph community succession during the VAHINE
707 mesocosm experiment (New Caledonia lagoon), *Biogeosciences*, 12, 7435–7452, 2015.

708 Von Friesen, L. W. and Riemann, L.: Nitrogen fixation in a changing Arctic Ocean: an overlooked source of nitrogen?, *Frontiers in Microbi-
709 ology*, 11, 596 426, 2020.

710 Wang, S., Bailey, D., Lindsay, K., Moore, J., and Holland, M.: Impact of sea ice on the marine iron cycle and phytoplankton productivity,
711 *Biogeosciences*, 11, 4713–4731, 2014.

712 Zehr, J. P. and Capone, D. G.: Changing perspectives in marine nitrogen fixation, *Science*, 368, eaay9514, 2020.